

In situ Monitoring of Vapor-phase Polymerization and Characterization of Poly(3,4-ethylenedioxythiophene) Thin Films

Yasuko Koshihara,¹ Mana Hirai,¹ Shohei Horike,¹ Masahiro Morimoto,^{1,3}
Masahiro Misaki,^{1,4} Tastuya Fukushima,¹ and Kenji Ishida^{1,2*}

¹Department of Chemical Science and Engineering, Graduate School of Engineering, Kobe University,
1-1 Rokkodai-cho, Nada, Kobe 657-8501, Japan

²Center for Membrane and Film Technology, Graduate School of Engineering, Kobe University,
1-1 Rokkodai-cho, Nada, Kobe 657-8501, Japan

³Graduate School of Science and Engineering for Research, University of Toyama,
3190 Gofuku, Toyama 930-8555, Japan

⁴Electrical and Electronic Systems Course, Department of Comprehensive Engineering,
Kindai University Technical College, 7-1 Kasugaoka, Nabari 518-0459, Japan

(Received May 10, 2018; accepted August 10, 2018)

Keywords: PEDOT, vapor-phase polymerization, *in situ* UV–Vis, thermoelectric conversion

Thin films of poly(3,4-ethylenedioxythiophene) (PEDOT) were fabricated via the vapor-phase polymerization (VPP) of the monomer 3,4-ethylenedioxythiophene (EDOT) with $\text{FeCl}_3 \cdot 6\text{H}_2\text{O}$ as the oxidant. The doping level and electrical properties of the VPP-PEDOT films were investigated by Raman spectroscopy, X-ray photoelectron spectroscopy (XPS), and electrical conductivity measurements. The VPP of EDOT was observed by *in situ* ultraviolet–visible (UV–Vis) absorption spectroscopy. The results showed that highly doped PEDOT films were formed in the initial stages of VPP, and the doping level increased as the reaction proceeded. The doping level eventually decreased because of the limited amount of the oxidant. Therefore, it was concluded that the doping level of VPP-PEDOT thin films could be changed depending on the initial amount and supply of the oxidant. The thermoelectric properties of the as-synthesized VPP-PEDOT films were also studied, with the aim of applying them as an energy harvester and/or a temperature sensor.

1. Introduction

Poly(3,4-ethylenedioxythiophene) (PEDOT) has attracted significant attention in recent years because of its high conductivity, outstanding chemical stability under ambient conditions, and transparency, and consequently has been used in various organic electronic devices.^(1–5) In addition, the thermoelectric power of PEDOT has also been reported.^(6–10) Thermoelectric devices harvest electricity from the heat generated from natural resources and are particularly useful for remote sensing applications in the Internet of Things (IoT).^(11–13) Moreover, thermoelectric materials can be applied to temperature sensors, because they generate electric

*Corresponding author: e-mail: kishida@crystal.kobe-u.ac.jp
<https://doi.org/10.18494/SAM.2018.1986>

voltage from a temperature gradient. In thermoelectric conversion, the performance of materials is defined using a thermoelectric figure of merit, $ZT = S^2\sigma T/\kappa$, where S , σ , and κ are the Seebeck coefficient, electrical conductivity, and thermal conductivity, respectively. These three parameters are dependent on each other; S has an inverse relationship with σ . It is worth noting that PEDOT shows particular promise for use as a thermoelectric material because its κ is low and its σ can be changed by chemical doping.

Generally, PEDOT is used with poly(4-styrenesulfonate) (PSS) as the dopant in the form of PEDOT:PSS. The PEDOT:PSS composite can be dispersed in water and its films can be easily prepared via the solution processing method. On the other hand, PEDOT thin films have also been fabricated by vapor-phase polymerization (VPP).^(10,14–18) The VPP technique is a bottom-up processing method^(14–19) by which the vapor of the monomer 3,4-ethylenedioxythiophene (EDOT) directly polymerizes at the surface of the oxidant layer. After the polymerization process, the counter anions of the oxidant remain in the PEDOT thin films as the PEDOT dopant. In the case of VPP-PEDOT films, high Seebeck coefficients have been reported,⁽⁷⁾ suggesting the importance of the VPP process in improving the thermoelectric performance. To control the oxidation level of VPP-PEDOT, it is crucial to be able to observe the VPP process. However, there are very few reports on the *in situ* monitoring of the VPP process. For example, Fabretto *et al.* have reported the *in situ* analysis of the VPP of PEDOT thin films using a quartz crystal microbalance with dissipation measurements.⁽²⁰⁾ However, they did not measure the absorption spectra.

Therefore, in this study, we focused on the VPP of PEDOT thin films and investigated their deposition by *in situ* absorption measurements. Then, the relationship between the reaction time and the doping level of the VPP-PEDOT thin films was investigated and the thermoelectric characteristics of the resulting materials were also evaluated.

2. Materials and Methods

The EDOT monomer and ferric chloride hexahydrate ($\text{FeCl}_3 \cdot 6\text{H}_2\text{O}$) were purchased from Tokyo Chemical Industry (Japan) and Nacalai Tesque (Japan), respectively. The PEDOT films were prepared by the VPP technique using $\text{FeCl}_3 \cdot 6\text{H}_2\text{O}$ as the oxidant. $\text{FeCl}_3 \cdot 6\text{H}_2\text{O}$ was dissolved in ethanol with a concentration of 5 wt%. This solution was then deposited on cleaned fused quartz and Si-wafer substrates by the spin-coating method and dried at 80 °C. After drying, the substrate coated with $\text{FeCl}_3 \cdot 6\text{H}_2\text{O}$ was immediately mounted in the quartz chamber, where the EDOT monomer was evaporated at 60 °C for 10–60 min. Finally, after the completion of the reaction, the substrate with the VPP-PEDOT film was rinsed with ethanol for 10 min to remove the oxidant and any unreacted monomer.

The absorption spectrum was recorded during the VPP reaction using a multichannel spectrometer (BAS; SEC2000). The VPP-PEDOT films were also examined by ultraviolet-visible-near-infrared spectroscopy (UV-Vis-NIR; JASCO V-670), Raman spectroscopy (JASCO NRS-7100), and X-ray photoelectron spectroscopy (XPS; ULBAC PHI X-tool). The morphologies of the films were evaluated by atomic force microscopy (AFM; SII SPI3800N). The electrical conductivities of the films were measured by the standard four-terminal method,

while the Seebeck coefficients were determined using a laboratory-made setup at 298 K in vacuum with a semiconductor parameter analyzer (Keysight Technologies, B1500A).

3. Results and Discussion

The as-spun yellow $\text{FeCl}_3 \cdot 6\text{H}_2\text{O}$ film turned blue after being heated in the quartz chamber with the EDOT monomer for 60 min at 60 °C [Fig. 1(c) inset]. Figure 1(a) shows the Raman spectrum of the VPP-PEDOT thin film obtained at an excitation wavelength of 532 nm. The bands related to symmetric $\text{C}_\alpha=\text{C}_\beta$ stretching at 1423 cm^{-1} , asymmetric $\text{C}=\text{C}$ stretching at 1501 cm^{-1} , $\text{C}_\beta-\text{C}_\beta$ stretching at 1365 cm^{-1} , $\text{C}_\alpha-\text{C}_\alpha$ inter-ring stretching at 1260 cm^{-1} , oxyethylene ring deformation at 990 cm^{-1} , and symmetric $\text{C}-\text{S}-\text{C}$ deformation at 693 cm^{-1} could all be assigned to PEDOT. The strong absorption peak related to symmetric $\text{C}_\alpha=\text{C}_\beta$ stretching at $\sim 1423 \text{ cm}^{-1}$ indicated the oxidation of VPP-PEDOT.^(18,21) The XPS spectrum [Fig. 1(b)] had peaks characteristic of carbon, oxygen, sulfur, and chlorine. The atomic concentrations of C, O, S, and Cl calculated from the areas of their respective peaks were 67.7, 18.7, 6.6, and 5.6%, respectively; these values are consistent with the atomic ratio of PEDOT. Although Fe from the oxidant ($\text{FeCl}_3 \cdot 6\text{H}_2\text{O}$) was removed during washing with ethanol after the polymerization process, Cl^- ions remained in the PEDOT thin films. These results suggest that the PEDOT thin films were doped with Cl^- .^(6,18,22) Figure 1(c) shows the UV-Vis-NIR absorption spectrum of the VPP-PEDOT thin film. The VPP-PEDOT film sample showed absorption bands in the wavelength region of 200–400 nm and broad absorptions in the wavelength region of 500–2000 nm. The absorptions at $\sim 900 \text{ nm}$ and above 1250 nm were attributed to polaron and bipolaron states, respectively.^(9,23,24) These results suggest that a highly doped VPP-PEDOT film was obtained when VPP was conducted for 60 min at 60 °C.

In order to monitor the polymerization reaction, UV-Vis absorption spectra were measured during the VPP process [Fig. 2(c)]. Figure 2(a) shows the time course of the UV-Vis absorption spectrum upon heating the reaction mixture at 60 °C from 1 to 60 min. Before heating (at 0 min, not shown), the absorption band corresponding to $\text{FeCl}_3 \cdot 6\text{H}_2\text{O}$ was observed at 300–400 nm. After heating for 1 min, the absorbance increased slightly in the wavelength region between 500 and 800 nm, and subsequently increased continuously during VPP. As the

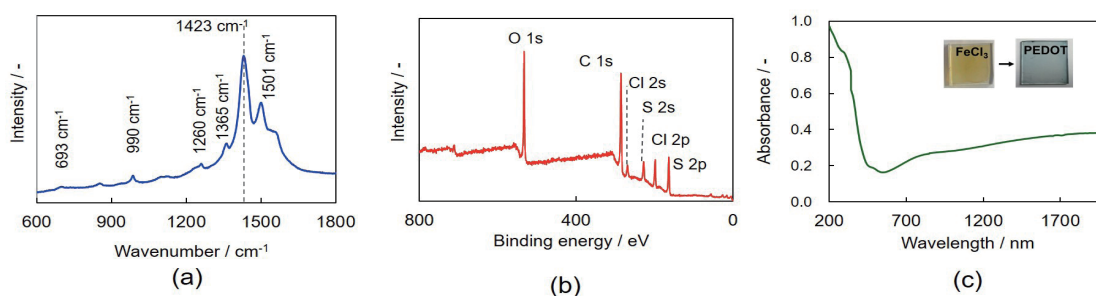


Fig. 1. (Color online) (a) Raman spectrum, (b) XPS spectrum, and (c) UV-Vis-NIR absorption spectrum of VPP-PEDOT thin film prepared at 60 °C for 60 min.

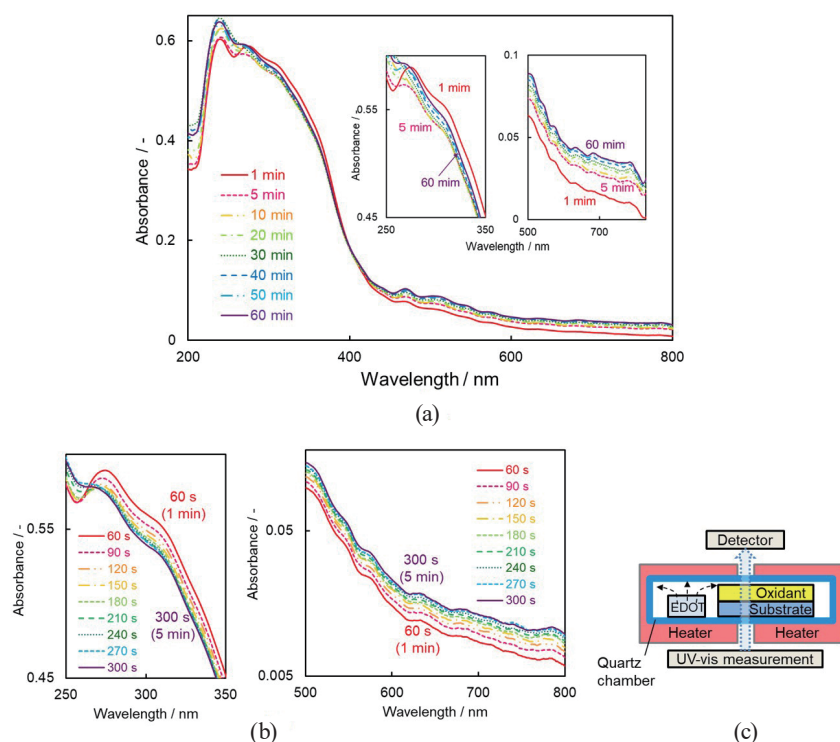


Fig. 2. (Color online) UV-Vis absorption spectra during VPP. (a) 1–60 min, (b) 60–300 s, and (c) experimental setup for *in situ* UV-Vis measurements.

gradual absorption from 500 nm into the IR region indicated a highly doped PEDOT sample, it was concluded that the VPP-PEDOT prepared in this study was doped within the first minute of the VPP process. The intensity of the band observed at 300–400 nm decreased dramatically at 5 min and only slightly from 5 to 20 min, and then increased again in the 20–60 min duration. This absorption region is related to not only $\text{FeCl}_3 \cdot 6\text{H}_2\text{O}$ but also to PEDOT. Therefore, in the initial 5 min, the intensity decreased with the decrease in the amount of $\text{FeCl}_3 \cdot 6\text{H}_2\text{O}$, while it increased after 20 min as PEDOT started to form. On the other hand, the absorption intensity in the region assignable to PEDOT (500–800 nm) increased sharply after 5 min of heating and continued to increase from 5 to 50 min. Therefore, the time course of the UV-Vis absorption spectrum was examined from 1 to 5 min [Fig. 2(b)].

The absorption in the range of 300–400 nm ($\text{FeCl}_3 \cdot 6\text{H}_2\text{O}$) decreased and that of 500–800 nm (PEDOT) increased sharply after 90 s of heating. These results indicated that FeCl_3 has a high redox activity, which leads to the rapid polymerization of EDOT and doping in PEDOT. In other words, highly doped PEDOT thin films were prepared in the initial stage of VPP.

Figure 3 shows AFM images of VPP-PEDOT films. The film prepared for a reaction time of 5 min was composed of grains with diameters of 70–100 nm [Fig. 3(a)]. After 20 min, the tighter layer that suggested polymer growth and some fissures were observed [Fig. 3(b)]. After 60 min, grooves with a depth of ~ 40 nm and a length of less than 1 μm were observed at the film surface [Fig. 3(c)]. Evans *et al.* have proposed a bottom-up PEDOT film growth mechanism during VPP. They described that the initial PEDOT layer with packed

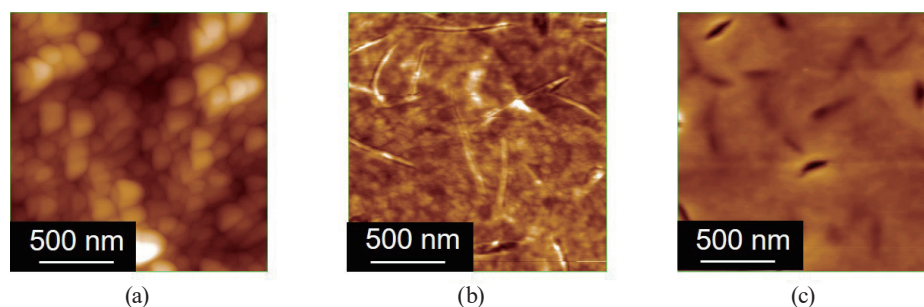


Fig. 3. (Color online) AFM images of VPP-PEDOT thin films formed at 60 °C for (a) 5, (b) 20, and (c) 60 min.

small polymer particles formed at the oxidant-vapor interface, and that the liquid oxidant was transported up to the surface through the granular PEDOT layer by the capillary mechanism.⁽²⁵⁾ In our experiment, the bottom-up growth of PEDOT films was suggested, because the oxidant ($\text{FeCl}_3 \cdot 6\text{H}_2\text{O}$) with a melting point of 37 °C was in the liquid state at 60 °C during VPP. On the other hand, Li *et al.* have reported that FeCl_2 remained on the PEDOT film after the VPP process and easily aggregated.⁽²⁶⁾ The fissures and grooves observed at the VPP-PEDOT surface were probably generated because of the loss of FeCl_2 during rinsing. After 5 min, the PEDOT film thickness remained unchanged at approximately 60 nm, which was comparable to the spin-coated oxidant thickness. These results suggest that the VPP-PEDOT film thickness depended on the thickness of the oxidant layer and increased rapidly in the initial 5 min during VPP.

In order to evaluate the variations in the oxidation state and electrical properties of VPP-PEDOT thin films at various reaction times, we estimated the doping level and measured the electrical conductivity. The doping level was calculated from the area ratio of the doped to undoped peaks of the thiophene S2p signal in the high-resolution XPS spectrum, using the shift of the S2p signal in response to the positive charges induced in the thiophene rings by the Cl^- dopant.^(15,26) As shown in Fig. 4(a), the doping level of the VPP-PEDOT films increased between 10 and 20 min, reached the maximum, and decreased beyond this time point. The conductivity measured with 1.0-mm-wide and 60-nm-thick VPP-PEDOT thin films increased drastically to a maximum of 2.3 S/cm at 20 min and then became approximately constant, as shown in Fig. 4(b). These conductivities are much lower than those of previously reported VPP-PEDOT thin films. The conductivity of the thin films was also found to be dependent on the film structure. In this case, from the AFM images, these film structures with many grooves were responsible for the low conductivity in the in-plane direction.

From the *in situ* UV-Vis measurement of EDOT polymerization and the evaluation of the doping level and conductivity of the VPP-PEDOT films, it was found that EDOT polymerized rapidly in the initial stages of VPP (1–5 min) and the oxidant was consumed proportionately. Up to 20 min, with continuous polymerization and doping with Cl^- , the doping level and consequently the conductivity of the PEDOT films also increased. Subsequently, the doping level decreased because the amount of the oxidant available was limited. However, the conductivity was higher than that at 10 or 15 min because the PEDOT chain length increased. These results suggest that the initial amount and supply of the oxidant are important in controlling the doping level of VPP-PEDOT films.

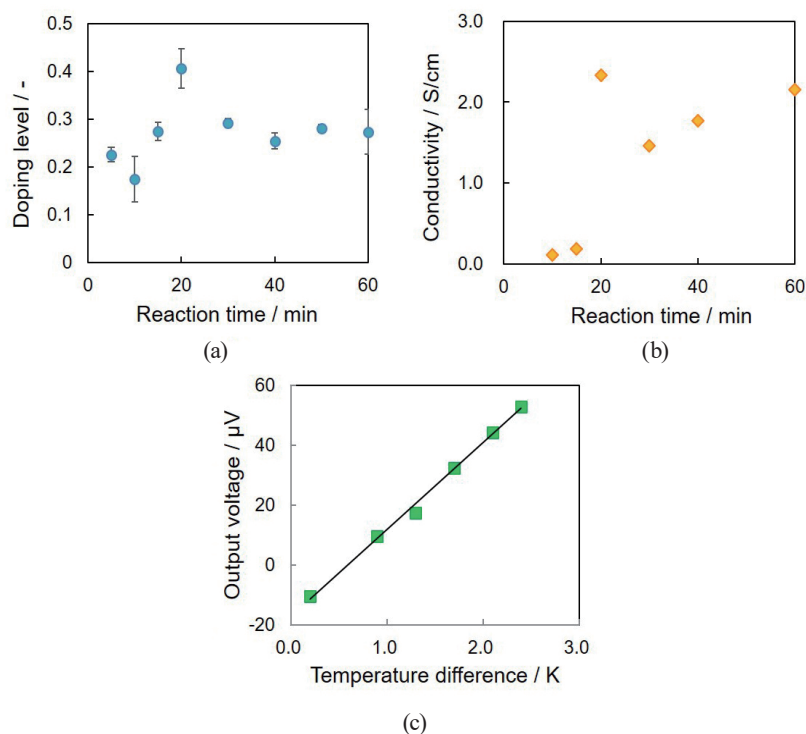


Fig. 4. (Color online) Relationship between reaction time and (a) doping level and (b) conductivity of VPP-PEDOT thin films; and (c) the thermoelectric properties of VPP-PEDOT thin film with 20 min reaction time.

The thermoelectric properties of the film formed with a reaction time of 20 min were evaluated. The temperature was measured using chromel–alumel thermocouples and the Seebeck coefficient was calculated from the $\Delta V/\Delta T$ slopes. The Seebeck coefficient of the VPP-PEDOT film at 300 K under vacuum was estimated to be 28.9 μ V/K from the linear output voltage versus temperature difference curve of the films [Fig. 4(c)]. This value is comparable to that previously reported for pristine PEDOT.⁽¹⁰⁾ As the focus of this study was simply to monitor the polymerization process, the VPP reaction conditions were not optimized. However, the *in situ* monitoring of the VPP process proved useful for examining the polymerization conditions necessary for fabricating PEDOT thin films for use as thermoelectric materials.

4. Conclusions

In this study, we investigated the fabrication of PEDOT thin films by VPP and characterized the obtained VPP-PEDOT thin films by AFM, UV–Vis–NIR absorption spectroscopy, Raman spectroscopy, and electric conductivity measurements. The PEDOT films doped with Cl were formed on oxidant-coated substrates upon heating the EDOT monomer for 60 min at 60 °C. The *in situ* monitoring of the polymerization of EDOT indicated that the monomer was rapidly polymerized and highly doped PEDOT was formed in the initial stages of VPP. It was also found that the doping level of the VPP-PEDOT films estimated from XPS spectra changed with

heating time because of the change in the amount of the oxidant available. In this experiment, the conductivity of the VPP-PEDOT film was low and the highest Seebeck coefficient was 28.9 $\mu\text{V}/\text{K}$. Therefore, it was proposed that the initial amount and supply of the oxidant were important in the control of the chemical doping of VPP-PEDOT during polymerization. *In situ* UV-Vis measurements of EDOT polymerization were useful for monitoring the VPP process, and the optimization of the VPP process led to the enhancement of the thermoelectric performance of the VPP-PEDOT thin films.

Acknowledgments

This work was partially supported by JSPS KAKENHI and Hyogo Science and Technology Association.

References

- 1 Y. Wang, C. X. Zhu, R. Pfattner, H. P. Yan, L. H. Jin, S. C. Chen, F. Molina-Lopez, F. Lissel, J. Liu, N. I. Rabiah, Z. Chen, J. W. Chung, C. Linder, M. F. Toney, B. Murman, and Z. Bao: *Sci. Adv.* **3** (2017) e1602076.
- 2 Y. H. Kim, C. Sachse, M. L. Machala, C. May, L. Müller-Meskamp, and K. Leo: *Adv. Funct. Mater.* **21** (2011) 1076.
- 3 T. Takano, H. Masunaga, A. Fujiwara, H. Okuzaki, and T. Sasaki: *Macromolecules* **45** (2012) 3859.
- 4 S. Kirchmeyer and K. Reuter: *J. Mater. Chem.* **15** (2005) 2077.
- 5 K. Sun, S. Zhang, P. Li, Y. Xia, X. Zhang, D. Du, F. H. Isikgor, and J. Ouyang: *J. Mater. Sci. Mater. Electron.* **26** (2015) 4438.
- 6 G.-H. Kim, L. Shao, K. Zhang, and K. P. Pipe: *Nat. Mater.* **12** (2013) 719.
- 7 O. Bubnova, Z. U. Khan, A. Malti, S. Braun, M. Fahlman, M. Berggren, and X. Crispin: *Nat. Mater.* **10** (2011) 429.
- 8 T. Park, C. Park, B. Kim, H. Shin, and E. Kim: *Energy Environ. Sci.* **6** (2013) 788.
- 9 J. Wang, K. Cai, and S. Shen: *Org. Electron.* **17** (2015) 151.
- 10 Y. Jia, X. Li, F. Jiang, C. Li, T. Wang, Q. Jiang, J. Hou, and J. Xu: *J. Polym. Sci., Part B: Polym. Phys.* **55** (2017) 1738.
- 11 H. Glosch, M. Ashauer, U. Pfeiffer, and W. Lang: *Sens. Actuators* **7** (1999) 246.
- 12 A. Dewan, S. U. Ay, M. N. Karim, and H. Beyenal: *J. Power Sources* **245** (2014) 129.
- 13 S. Horike, T. Fukushima, T. Saito, T. Kuchimura, Y. Koshiba, M. Morimoto, and K. Ishida: *Mol. Syst. Des. Eng.* **2** (2017) 616.
- 14 M. Fabretto, K. Zuber, C. Hakll, and P. Murphy: *Macromol. Rapid Commun.* **29** (2008) 1403.
- 15 B. Cho, K. S. Park, J. Baek, H. S. Oh, Y.-E. K. Lee, and M. M. Sung: *Nano Lett.* **14** (2014) 3321.
- 16 B. Winther-Jensen, O. Winther-Jensen, M. Forsyth, and D. R. MacFarlane: *Science* **321** (2008) 671.
- 17 J.-Y. Kim, M.-H. Kwon, Y.-K. Min, S. Kwon, and D.-W. Ihm: *Adv. Mater.* **19** (2007) 3501.
- 18 J. M. D'Arcy, M. F. El-Kady, P. P. Khine, L. Zhang, S. H. Lee, N. R. Davis, D. S. Liu, M. T. Yeung, and S. Y. Kim: *ACS Nano* **8** (2014) 1550.
- 19 Y. Koshiba, M. Nishimoto, A. Misawa, M. Misaki, and K. Ishida: *Jpn. J. Appl. Phys.* **55** (2016) 03DD07.
- 20 M. Fabretto, M. Müller, C. Hall, P. Murphy, R. D. Short, and H. J. Griesser: *Polymer* **51** (2010) 1737.
- 21 W. W. Chiu, J. Travaš-Sejdić, R. P. Cooney, and G. A. Bowmaker: *J. Raman Spectrosc.* **37** (2006) 1354.
- 22 H. Yan and H. Okuzaki: *Synth. Mater.* **159** (2009) 2225.
- 23 T. C. Chung, J. Kaufman, A. Heeger, and F. Wudl: *Phys. Rev. B* **30** (1984) 702.
- 24 S. Garreau, J. L. Duvail, and G. Louarn: *Synth. Met.* **125** (2001) 325.
- 25 D. Evans, M. Fabretto, M. Mueller, K. Zuber, R. Shorta, and P. Murphy: *J. Mater. Chem.* **22** (2012) 14889.
- 26 Y. Li, X. Hu, S. Zhou, L. Yang, J. Yan, C. Suna, and P. Chen: *J. Mater. Chem. C* **2** (2014) 916.